Supporting Information

Jenouvrier *et al.* 10.1073/pnas.0806638106

SI Text

Selection of IPCC Climate Models. We used sea ice extent averaged over a sector between the longitude 120°E and 160°E. This sector is centered on Dumont d'Urville (66′40°S, 140′01°E) where the emperor penguin colony is located. This sector includes the foraging area of emperor penguin in Terre Adélie (16), and a surrounding area within which large scale sea ice effects on the food web are likely. We explored other choices of spatial resolution; Fig. S2 shows that the statistical properties of sea ice extent from small (135°E–145°E) to large spatial scales (120°E and 160°E) are similar. From the original 16 GCMs, we selected 10 models whose output agrees with the observed Antarctic sea ice data. We removed models CGCM3.1(T63), GISS-AOM, and CCSM3 because they produced a mean SIE at least 50% higher than the observed mean during winter (July to September) between 1978 to 2007. We removed models GISS-ER and ECHO-G because they produced a mean at least 50% lower than the observed mean (Fig. S3). Finally, we removed model INM-CM3.0 because it does not include dynamic processes for modeling sea ice (see more information on the models at www.pcmdi.llnl.gov/ipcc/model_documentation).

As shown by Table S1, the observed sea-ice trend in our study area is at present slightly positive, and 4/10 of our selected models show such a trend for the 1979–2006 time period. The 10 selected models predict a range of trends over the 21st century in winter SIE in Terre Adélie ranging from very little change (0.1% per decade for model IPSL-CM4) to a strong negative trend (−3.7% per decade for model MRI-CGCM2.3.2) (see Table S1). By using 10 GCMs we account for some of the uncertainties related to any single climate projection.

Consequences of a Binary Environment Model

Stochastic growth depends on the relation between the environment and the vital rates. Our 2-state environment model simplifies that relationship. It does so in a biologically reasonable way, approximating the expected sigmoid response of the vital rates with a Heaviside function. A reviewer questioned our results might be an artifact of the simplification from a continuous to a discrete environment. To investigate this, we constructed what may be the simplest continuous-environment model compatible with our observations. It includes a linear dependence of the entries of the population projection matrix $\mathbf{A}$ on the proportional SIE anomaly x, obtained by interpolating between the observed matrices for normal and warm conditions. This linear function can produce mathematically impossible results, and so must be constrained at the extremes. We imposed the following constraints on $\mathbf{A}[x(t)]$. First, all matrix entries must be non-negative. If any entries became negative, they were set to 0. Second, emperor penguins cannot produce more than a single offspring. Thus, if fertility ever exceeded 0.5, it was set to 0.5. Third, no new individuals should be produced by the transitions and survival of already existing individuals. This required that

$$\sum_{j=2}^{7} a_{ij}[x(t)] \leq 1 \text{ for } i = 1,\cdots,7.$$

If this sum ever exceeded 1, we rescaled the column of the matrix to sum to 1.

Each of the 10 IPCC climate model produces a single time series $x(t)$ for $t = 2000, 2001, \ldots, 2100$. The demography is described by: $\mathbf{n}(t+1) = \mathbf{A}[x(t)]\mathbf{n}(t)$, where the matrix $\mathbf{A}[x(t)]$ projects the population vector $\mathbf{n}$ from t to $t+1$, according to the proportional SIE anomalies x at time t. For each climate model, we created an initial population in the year 2000 with the stable stage distribution and average number of breeding pairs over the period 1982–2005. This approach necessarily treats the IPCC model output as a deterministic, because stochastic climate projections for each IPCC model are not available.

Fig. S4 shows the results. All 10 IPCC models predict a decline in the penguin population by the end of the century. The median of the 10 projections declined from 3,000 to 3 breeding pairs. These results are qualitatively the same as our binary-environment model, but quantitatively more extreme than those produced by the binary environment model. Because the continuous model requires extrapolation of the SIE dependence of the vital rates beyond the observed range of variation, its results are unreliable, but it shows that the model based on the 2-state environment produces conservative results.

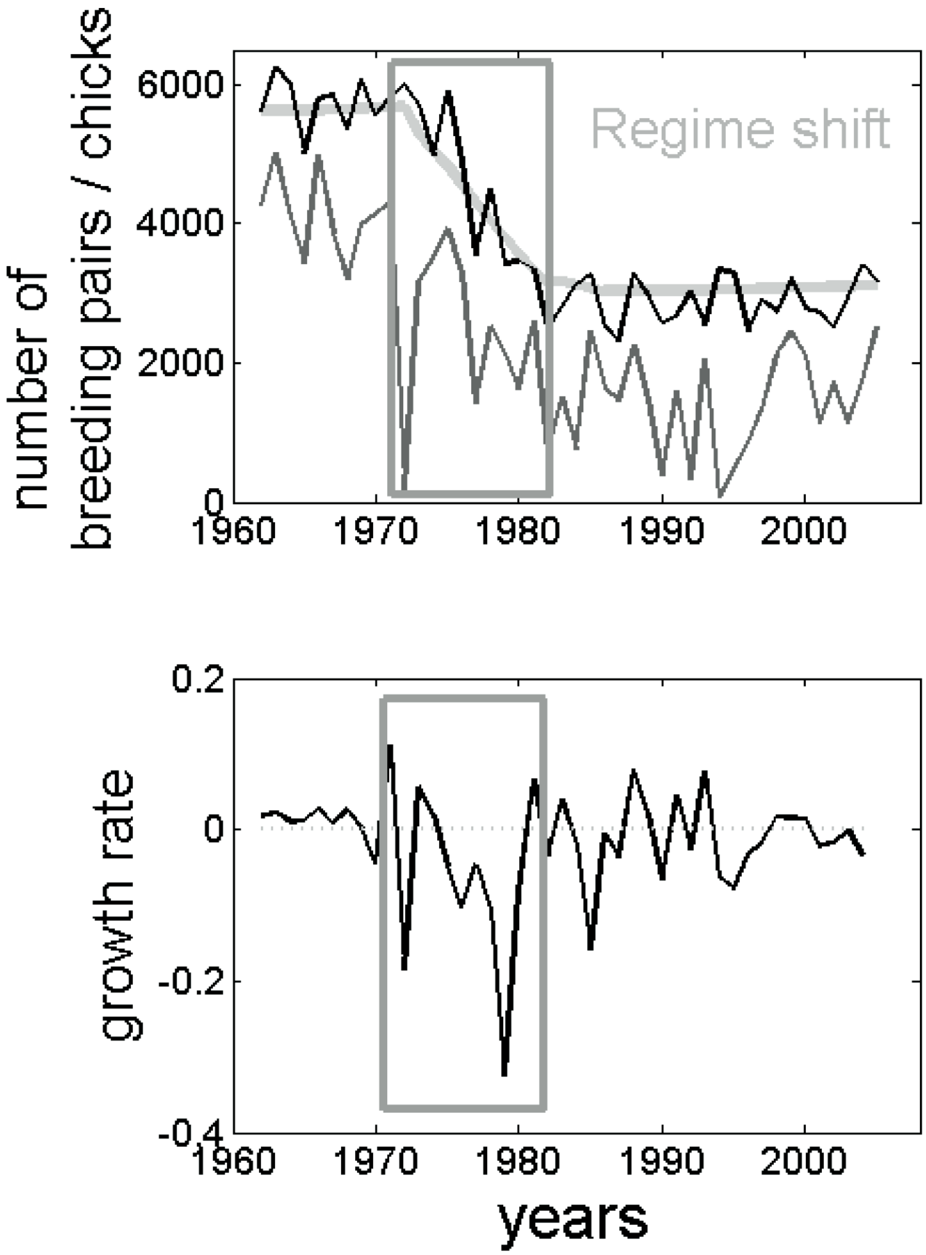

Fig. S1. (*Upper*) The number of breeding pairs (black line) and chicks (gray line) of the emperor penguin in Terre Adélie, Antarctica, between 1962 and 2005. The thick light gray line gives the number of breeding pairs calculated by a deterministic matrix model with 2-states, with warm and regular environmental conditions during and outside the regime shift periods respectively. (*Lower*) The rate of increase of the population calculated as the log of the deterministic growth rate. The rectangle identifies the period of the regime shift.

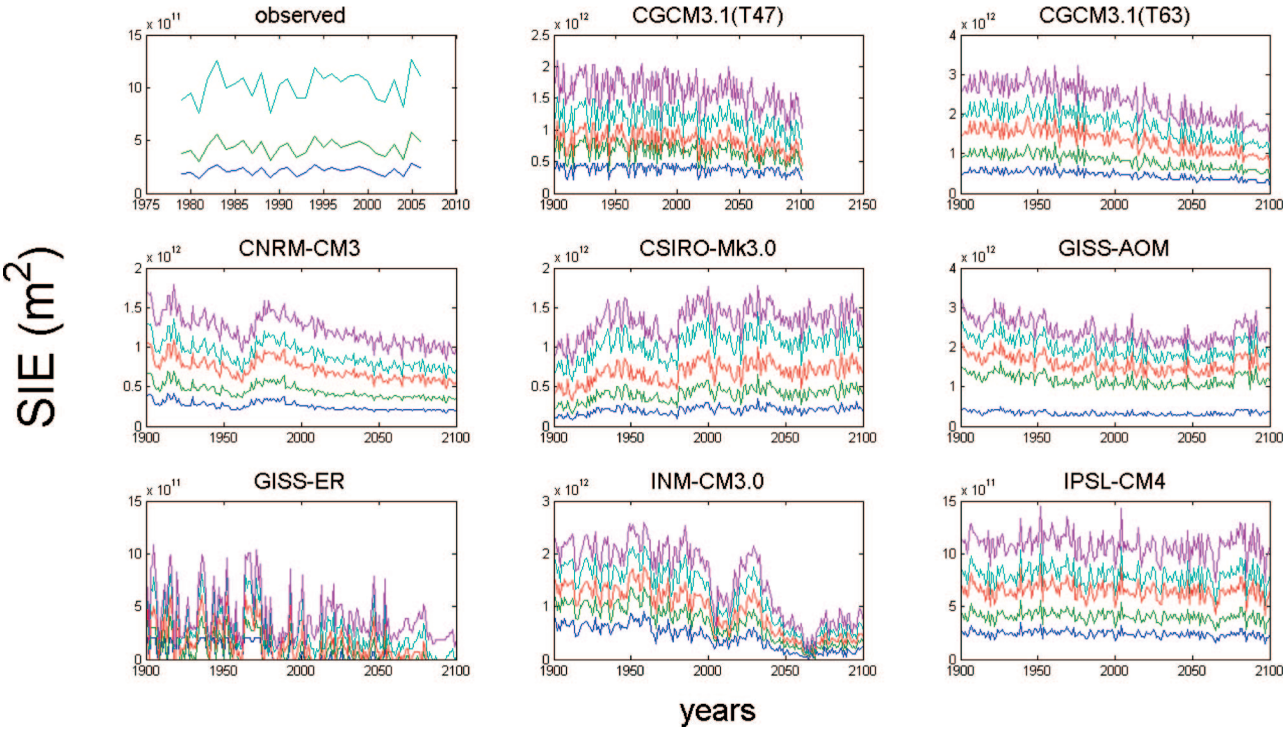

Fig. S2. Sea ice extent (m^2) during winter over different spatial sectors centered on Dumont d'Urville (66′40°S, 140′01°E), Antarctica, between 1979 and 2006 for the satellite observation, and between 1900 and 2099 for each of the IPCC climate models.

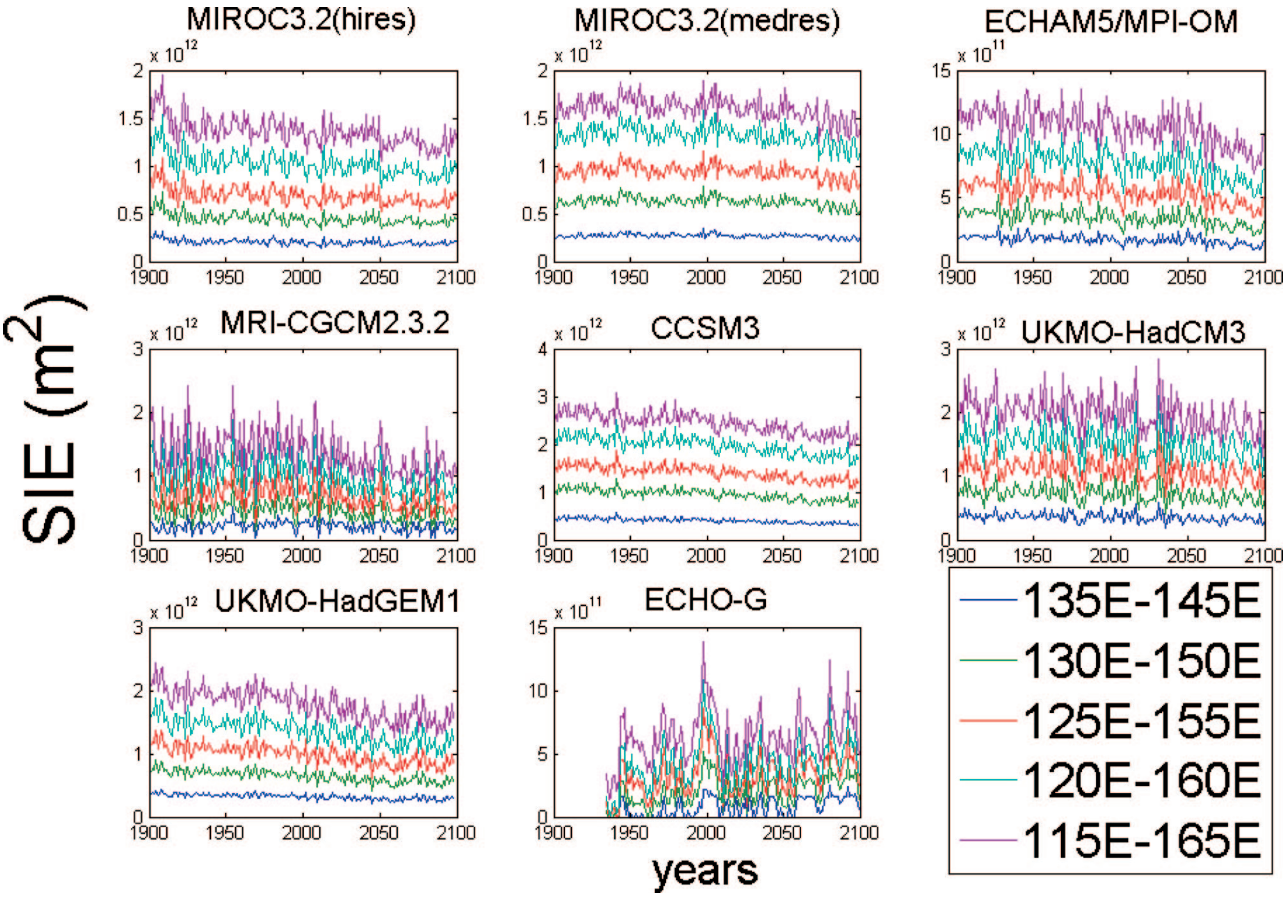

Fig. S2 (continued).

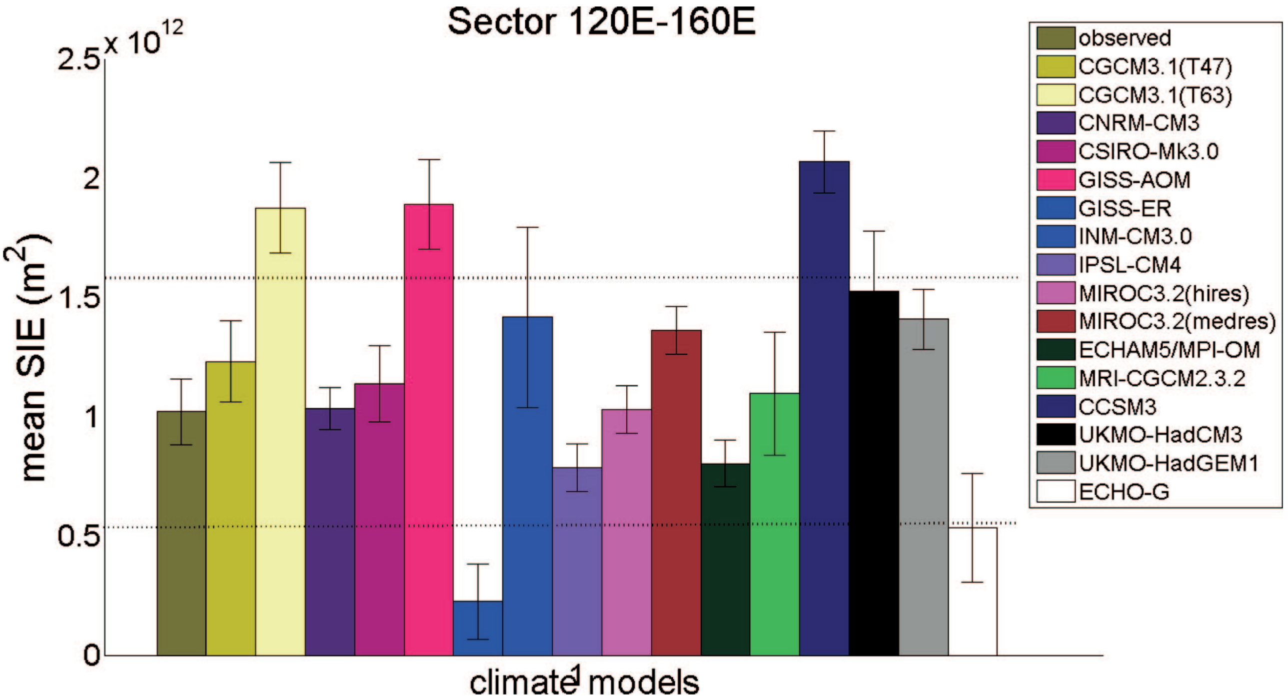

Fig. S3. Mean sea ice extent (m^2) during winter over the sector between 120°E and 160°E in Terre Adélie, Antarctica, during 1979–2006, for the observed satellite data (dark green) and from 16 IPCC climate model (see legends). The error bars indicate the interannual variability in sea ice extent. The dotted lines represent values 50% higher or lower than the observed satellite data mean. The models that were outside these two dotted lines were eliminated from our analysis.

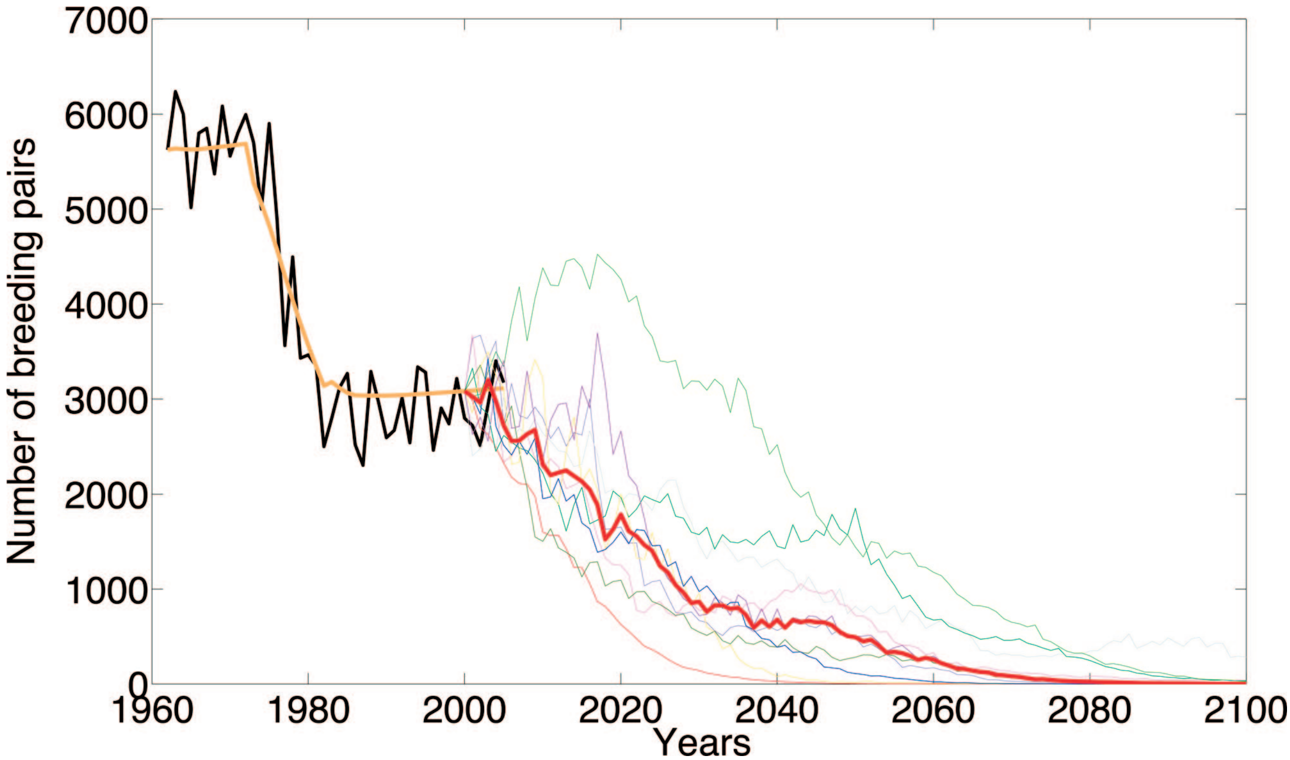

Fig. S4. Observations and projections of the emperor penguin population. Population projections come from a deterministic population model in which the vital rates are a continuous linear function of SIE, obtained by interpolating between the projection matrices in warm and normal conditions. The projections are based on the SIEa forecasts produced by the 10 IPCC models; thin line colors as in Fig. 2. The thick dark line is the observed number of breeding pairs. The thick orange line from 1962 to 2000 is the projected number of breeding pairs based on the observed sequence of warm events. The thick red line from 2005 to 2100 is the median of 10 projections based on the IPCC projections of SIE.

Table S1. Information about the climate models from the Intergovernmental Panel on Climate Change (IPCC) assessment report that we used in our analysis

Sources	Modeling groups	Country	Present SIE trend	Future SIE trend
Observation	National Snow and Ice Data Center	USA	2.93	
	Climate models used in our analysis			
CGCM3.1(T47)	Canadian Centre for Climate Modelling and Analysis	Canada	−0.96	−2.45
CNRM-CM3	Météo-France-Centre National de Recherches Météorologiques	France	−8.34	−2.79
CSIRO-Mk3.0	CSIRO Atmospheric Research	Australia	4.64	−0.18
IPSL-CM4	Institut Pierre Simon Laplace	France	5.75	0.14
MIROC3.2(hires)	Center for Climate System Research (The University of Tokyo), National Institute for Environmental Studies, and Frontier Research Center for Global Change (JAMSTEC)	Japan	−4.89	−1.37
MIROC3.2(medres)	Center for Climate System Research (The University of Tokyo), National Institute for Environmental Studies, and Frontier Research Center for Global Change (JAMSTEC)	Japan	4.14	−1.71
ECHAM5/MPI-OM	Max Planck Institute for Meteorology	Germany	−1.66	−2.74
MRI-CGCM2.3.2	Meteorological Research Institute	Japan	−5.73	−3.71
UKMO-HadCM3	Hadley Centre for Climate Prediction and Research/Met Office	UK	3.72	−1.63
UKMO-HadGEM1	Hadley Centre for Climate Prediction and Research/Met Office	UK	−3.97	−1.91
	Climate models excluded from our analysis			
CGCM3.1(T63)	Canadian Centre for Climate Modelling and Analysis	Canada	−3.53	−3.98
GISS-AOM	NASA Goddard Institute for Space Studies	USA	−4.13	1.31
GISS-ER	NASA Goddard Institute for Space Studies	USA	17.08	−11.74
INM-CM3.0	Institute for Numerical Mathematics	Russia	−23.31	−13.37
CCSM3	National Center for Atmospheric Research	USA	−3.43	−1.52
ECHO-G	Meteorological Institute of the University of Bonn and Meteorological Research Institute of KMA	Germany and Korea	39.70	5.45

The present winter SIE trend during the satellite period of 1979–2006 and the future trend for the period of 2006–2098 are calculated for a sector between 120E and 160 E in Terre Adélie, Antarctica. Trends are measured in % per decade. More information on the models is available from http://www-pcmdi.llnl.gov/ipcc/model_documentation. The 6 climate models excluded from our analysis are at the bottom of the table.

Table S2. Population projection matrices, A_N and A_W, for normal and warm conditions, as averages of annual matrices outside and inside the regime shift, respectively

Normal conditions	PB-1	PB-2	PB-3	PB-4	PB-5	NB	B
PB-1	0	0	0	0	0	0	0.2291
PB-2	0.9064	0	0	0	0	0	0
PB-3	0	0.852	0	0	0	0	0
PB-4	0	0	0.7432	0	0	0	0
PB-5	0	0	0	0.6889	0.7971	0	0
NB	0	0	0	0	0	0.179	0.179
B	0	0.0544	0.1632	0.2175	0.1093	0.7274	0.7274
Warm conditions	PB-1	PB-2	PB-3	PB-4	PB-5	NB	B
PB-1	0	0	0	0	0	0	0.1487
PB-2	0.8689	0	0	0	0	0	0
PB-3	0	0.8168	0	0	0	0	0
PB-4	0	0	0.7125	0	0	0	0
PB-5	0	0	0	0.6604	0.7724	0	0
NB	0	0	0	0	0	0.1954	0.1954
B	0	0.0521	0.1564	0.2085	0.0965	0.6735	0.6735

The 7 stages of the population are specified, with the 5 age classes of pre-breeders (PB-*i* for age *i*), non-breeding (NB) and breeding adults (B).